Biochimica et Biophysica Acta, 776 (1984) 217–227
Elsevier

BBA 72221

INTERACTION OF ANTIBODIES WITH LIPOSOMES BEARING FLUORESCENT HAPTENS

ASHOT PETROSSIAN and JOHN C. OWICKI *

Department of Biophysics and Medical Physics, University of California, Berkeley, and Division of Biology and Medicine, Lawrence Berkeley Laboratory, University of California, Berkeley, CA 94720 (U.S.A.)

(Received February 21st, 1984)

Key words: Membrane-antibody interaction; Fluorescein-lipid hapten; Liposome; Lipid composition; Kinetics; Fluorescence

Kinetic and equilibrium aspects of the recognition of antigenic model membranes by antibodies have been studied. Monoclonal anti-fluorescein IgG and its monovalent Fab fragment were allowed to interact with a fluorescein-lipid hapten that was incorporated into phospholipid vesicles. The binding was assayed in the nanomolar hapten concentration range by monitoring the quenching of hapten fluorescence by antibody. The rate and strength of the binding depended on the lipid composition of the vesicles; cholesterol enhanced both. The biphasic binding kinetics observed at high antibody concentrations for some compositions, plus additional spectroscopic evidence, led us to hypothesize that the hapten existed in a composition-dependent equilibrium between at least two conformations: (1) extended away from the membrane surface, available for binding, and (2) sequestered at or in the surface, unavailable for binding. The rate and strength of IgG binding were always greater than those of Fab, indicating bivalent binding by the IgG. This binding was intra-vesicular, since no agglutination of the vesicles was detected.

* To whom correspondence should be addressed.

Abbreviations:

Cbz,	carbobenzyloxyl
5-DCTAF,	5-dichlorotriazinylaminofluorescein
DEPC,	dielaidoylphosphatidylcholine
DMPC,	dimyristoylphosphatidylcholine
DOPC,	dioleoylphosphatidylcholine
DPhPC,	diphytanoylphosphatidylcholine (di-3,7,11,15-tetramethylhexadecanoyl-PC)
DPPC,	dipalmitoylphosphatidylcholine
DPPE,	dipalmityolphosphatidylethanolamine
FG_3P,	fluorescein-chlorotriazinyl-triglycyl-DPPE
IgG,	immunoglobulin G
NMR,	nuclear magnetic resonance
PAGE,	polyacrylamide gel electrophoresis
PC,	phosphatidylcholine
PE,	phosphatidylethanolamine
POPC,	1-palmitoyl-2-oleoylphosphatidylcholine
SDS,	sodium dodecyl sulfate
SIMS,	secondary-ion mass spectroscopy
TLC,	thin-layer chromatography

Introduction

Our laboratory is engaged in a detailed analysis of the interactions of IgG and monovalent Fab fragments with haptens that are covalently attached to lipids and then incorporated into phospholipid vesicles (liposomes). Our motivations for choosing such a model system are diverse.

First, one's ability to define and control the properties of liposomes makes them ideal for studying many basic biological questions [1–3]. In this paper we are investigating how antibody multivalency and the physico-chemical properties of membranes influence immune recognition. Other immunological studies involving liposomes have ranged from the discovery in Kinsky's laboratory that vesicles containing haptenated lipids are immunogenic [4], to investigations of the mechanism

of activation of the serum complement cascade [5] and the IgE-mediated degranulation of basophils [6].

Second, small antigenic moieties covalently bound to lipids (total molecular weight 1000 to 3000) are biologically important, and the significance of this group of compounds is becoming increasingly evident. One example is given by the glycosphingolipids [7], which have importance as blood group antigens [8], as receptors for bioactive factors such as cholera toxin [9], and in oncogenic tranformation [10], and immunological recognition [11–15].

Finally, haptenated vesicles also have direct clinical and technological applications. For example, vesicles to which antibodies have been affixed and whose aqueous interiors are loaded with drugs are being tested as specifically targeted vectors for chemotherapy [16–19]. Vesicles also have potential in extremely sensitive analytical immunoassays: there is a large signal amplification inherent in attaching a small number of molecules to be assayed to a large structure such as a vesicle that can contain many indicator molecules, e.g., radioisotopes or spectroscopic probes [20–22].

In designing our model system, we chose a fluorescent moiety, fluorescein, as a hapten. Fluorescein is highly immunogenic, and this large hapten approximates the space-filling properties of a normal antigenic determinant [23]. Antibodies against fluorescein efficiently quench its fluorescence, permitting convenient binding assays at or below nanomolar hapten concentrations [24–26]. Monoclonal antibodies with a range of affinities and isotypes have been raised against fluorescein, and the antibody-hapten interactions have been well studied [27,28]. The idiotypic properties of murine anti-fluorescein antibodies have been studied recently [29]. Another advantage is that the spectroscopic properties of fluorophores such as fluorescein are sensitive to the chemical environment, concentration, and motion of the probe. This permits important analyses of the state of the model system in the absence of antibody [30].

Our molecule, FG_3P (Fig. 1), is of the form hapten-spacer-lipid, where fluorescein is the hapten, a chlorotriazinyl linker plus triglycine form the spacer, and DPPE is the lipid. The spacer is necessary because when haptens are attached too close to the membrane surface, liposomal immunological reactivity is low [31,32]. Haptens that can project more deeply into the antibody binding site confer more reactivity. When fully extended, our spacer is about 1.3 nm long (measuring from the nitrogen on DPPE to the base of the fluorescein ring).

Materials and Methods

Chemicals. Unless otherwise noted, chemicals were obtained from Sigma Chemical Co. (St. Louis, MO) and were used without further purification.

Lipids and haptens. DMPC, DPPC, DPhPC, and the haptenated lipid fluorescein-PE were obtained from Avanti Polar Lipids (Birmingham, AL). Egg-yolk PC was purchased from GIBCO Laboratories (Grand Island, NY). 5-DCTAF was purchased from Research Organics (Cleveland, OH).

Synthesis of haptenated lipid, FG_3P (Fig. 1). The synthesis will be described in detail elsewhere (Petrossian, Kantor, and Owicki, manuscript in preparation). A brief description follows here.

N-Cbz-glycylglycylglycine (Bachem, Torrance, CA) was activated with isobutyl chloroformate, and the product was reacted with DPPE. After removal of the Cbz group by catalytic hydrogenation, the product, glycylglycylglycyl-DPPE, was purified by TLC. Reaction of this with 5-DCTAF gave the final haptenated lipid, FG_3P (Fig. 1), which was again purified by TLC. The identity of the molecule was confirmed by proton NMR and by secondary-ion mass spectroscopy (SIMS).

Buffer. Unless otherwise noted, experiments were performed in borate-buffered saline (BBS), which was made from 20 mM sodium borate adjusted to pH 8.5 with HCl, with NaCl added to give a final osmolarity of 310 mosM. The buffer pH is a compromise between physiological accuracy and the analytical convenience of working at a high pH, where the hapten is fully ionized [30].

Antibody. Hybridoma line No. 4-4-20, which secretes a high-affinity anti-fluorescin IgG_{2a}, was obtained from E. Voss, Jr. [28]. Antibody was harvested from ascites fluid of BALB/c mice that had been primed with pristane [33,34]. Purification was done on a protein-A Sepharose affinity column [35] (Pharmacia Fine Chemicals, Piscataway,

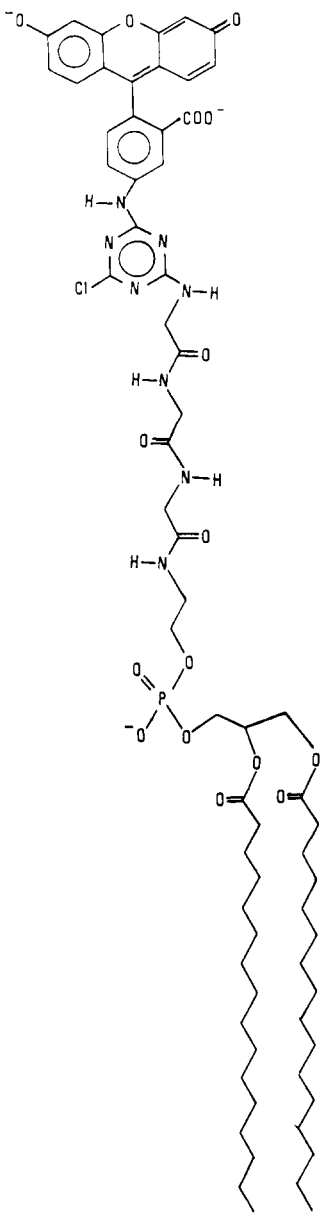

Fig. 1. Structure of the fluorescent lipid hapten FG_3P.

NJ), with elution at pH 3.0. One-dimensional SDS slab-gel PAGE using a 2.5–27% gradient gel (Isolab, Akron, OH) revealed one band. The identity of the antibody was confirmed by radial immunodiffusion against a serum specific for murine IgG_2 (a gift from A. Good).

Fab fragments. Monovalent Fab fragments were prepared by a modification of the method of Porter [36]. Briefly, 10 ml of solution was prepared that was 5.5 μM in IgG, 4.4 μM in papain, 5.0 mM in cysteine, and 100 mM in sodium phosphate (pH 7.5). This was stirred under argon for 5 h at 36 °C; the digestion was terminated by adding iodoacetamide (to 1.4 mM) and cooling on ice for 30 min. The digest was dialyzed and concentrated against 5 mM Tris-HCl (pH 8.0) at 4 °C.

The mixture was transferred to a protein-A Sepharose affinity column, which was washed successively with borate-buffered saline, 100 mM sodium acetate (pH 4.8), and 100 mM sodium acetate (pH 3.0). Fluorescein binding activity eluted with the second solution (pH 4.8). SDS-PAGE performed on this fraction revealed about equal amounts of two fragments with molecular masses of approx. 40 and 60 kDa. No intact antibody was detectable, nor was precipitation detectable by radial immunodiffusion, performed as above. The polyclonal anti-IgG_2 serum used in the immunodiffusion assay had much higher titer against Fc than Fab determinants, so the negative result is a good indication of the absence of Fc in our preparation.

Phospholipid vesicles. Vesicles were prepared by the ethanol-injection method [37,38]. 100 μl of 25 mM lipid in ethanol, containing 0.1 mol% FG_3P, was injected into 3.0 ml borate-buffered saline at 70 °C at a rate of 0.1 ml/min, with stirring. 3 min after the completion of the injection, the suspension was diluted 300-fold in borate-buffered saline at room temperature.

Vesicle morphology was analyzed by negative-stain electron microscopy. Vesicles were made in ammonium acetate buffer (pH 7.4) 310 mosM, stained with the same buffer containing 2.5% ammonium molybdate (iso-osmotic conditions), and observed with a Zeiss EM-952 electron microscope. The apparent diameter ($\pm$S.D.) of DPPC vesicles in the micrographs was 60 ± 15 nm. DPPC/cholesterol (2 : 1) vesicles were larger and more heterogeneous, with diameters in the range 85 ± 43 nm.

Assuming a surface area per lipid of roughly 0.6 nm^2, and interpreting the electron-microscopy results as the diameters of spheres, a typical DPPC vesicle had about 20 haptens on its outer monolayer. A typical DPPC/cholesterol (2 : 1) vesicle had about twice as many.

Fluorescence measurements. All fluorescence measurements were made on a microprocessor-controlled Fluorolog 2 (Spex Industries, Methuen, NJ) with double monochromators on excitation and emission. For analyzing binding, the excitation and emission wavelengths were 485 and 520 nm, unless otherwise specified. The sample temperature was controlled at 25 ± 1°C. Kinetic measurements were made by injecting up to 100 μl of IgG or Fab solution into 3.00 ml of a vigorously stirred vesicle suspension. Mixing time was about 2 s. In equilibrium studies, varying amounts of IgG or Fab were added to separate 2.00 ml samples of vesicles in cuvettes. After one to two hours of equilibration the fluorescence of each sample was measured.

Light-scattering measurements. The intensity of scattered light was measured at 410 m in the spectrofluorometer. The scattering angle was 90°. A correction was made for background scattering from the buffer and antibody preparation.

Analysis of binding equilibria. Equilibrium binding of IgG and Fab to sodium fluorescein was analyzed according to the reaction

$$B + F \rightleftharpoons BF \qquad (1)$$

where B is the binding site for hapten on the IgG or Fab and F is the fluorescein hapten. All IgG and Fab concentrations reported in this paper are binding-site concentrations. Affinity constants and IgG or Fab concentrations were determined by a nonlinear least-squares computer algorithm that was applied to the dependence of hapten fluorescence on the amoung of IgG or Fab added to the sample. This was easier to apply that graphical methods and also facilitated error analysis for the derived quantities.

Results

Binding equilibrium between sodium fluorescein and IgG or Fab

Aliquots of sodium fluorescein with concentrations 6.0 nM and 0.60 nM were titrated with IgG; see Fig. 2. The quenching curves were simultaneously fit to Reaction 1 as described above. Best-fit values of K, the equilibrium constant for the binding, and B_t, the binding-site concentration in the stock IgG titrant solution, are reported in Table I.

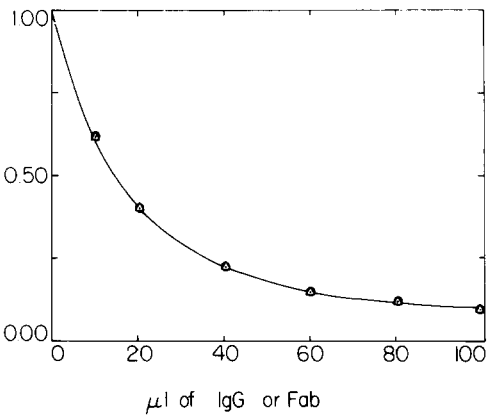

Fig. 2. Fluorescence (as fraction of initial fluorescence F_0) of a solution of sodium fluorescein (6.0 nM, 3.00 ml) titrated with IgG (△) and Fab (⊙).

The titration was repeated with a Fab solution adjusted to have the same sodium fluorescein-quenching ability as the IgG solution above. Again, see Fig. 2 and Table I. Since the affinities and concentrations of IgG and Fab in Table I are equal within experimental error, a third fitting was done using all four titrations to obtain a single K and B_t.

TABLE I

AFFINITY CONSTANTS AND BINDING-SITE CONCENTRATIONS FOR INTERACTION OF STOCK IgG AND Fab SOLUTIONS WITH SODIUM FLUORESCEIN

Affinity constants (K) and binding-site concentrations (B_t) were determined by fitting simulataneously the quenching curves (fluorescence vs. μl IgG or Fab) of solutions of 6.0 and 0.60 nM sodium fluorescein, using a nonlinear least-squares algorithm. The 'combined' values were obtained by fitting IgG and Fab data simultaneously. The reported ranges of values represent the 95%-confidence limits, based on a chi-square analysis.

Molecules	K (M^{-1}) ($\times 10^{-8}$)	B_t (M) ($\times 10^{6}$)
IgG	$4.00^{+1.20}_{-0.80}$	$1.44^{+0.28}_{-0.22}$
Fab	$4.34^{+1.10}_{-1.00}$	$1.40^{+0.25}_{-0.20}$
Combined	$4.20^{+1.10}_{-1.00}$	$1.42^{+0.30}_{-0.20}$

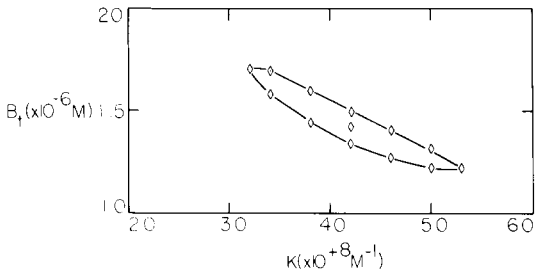

Fig. 3. Contour within which the binding-site concentration of the antibody preparation (B_t) and affinity of the binding site for sodium fluorescein (K) lie, at 95% confidence level. The contour is based on a chi-square analysis of computer fits to binding data such as that in Fig. 2. The central point is the global best fit.

The error limits for these quantities, at a 95% confidence level, were obtained from a chi-square analysis assuming an uncertainty of 1% of the full-scale fluorescence intensity for each titration curve. Fig. 3 shows the high correlation between uncertainties in K and B_t. It displays the 95%-confidence contour as a function of the presumed values of K and B_t simultaneously. If either parameter is fixed, the uncertainty in the other is much smaller than that reported in Table I.

Specificity of antibody binding to haptenated vesicles

Nonspecific IgG (a monoclonal murine anti-nitroxide IgG_2) failed to quench the fluorescence of haptenated vesicles. The anti-fluorescein IgG bound to vesicles only in the presence of hapten. This was shown by centrifugal separation of large unilamellar vesicles, made with and without FG_3P, from a solution containing the IgG, followed by a micro-protein assay (Kantor, A., and Petrossian, A., unpublished results). Finally, the IgG was unable to bind hapten that was held too close to the surface of the membrane: it was unable to quench the fluorescence of vesicles containing fluorescein-PE (which lacks a spacer between the hapten and headgroup).

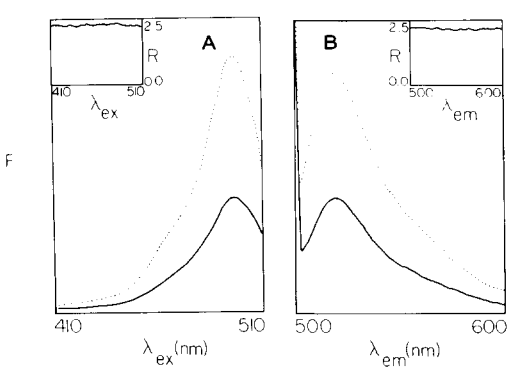

Fig. 4. Fluorescence excitation (A) and emission (B) spectra of 2.8 nM FG_3P in DPPC/cholesterol (2:1) vesicles. Spectra are taken without antibody (dotted lines) and after saturation of the vesicle surfaces with 67 nM antibody (solid lines). The insets are the ratios R of fluorescence without:with antibodies. Excitation and emission wavelengths were 495 nm and 515 nm.

Fluorescence spectra of bound and unbound haptenated vesicles

Excitation and emission spectra of FG_3P in vesicles composed of DPPC/cholesterol (2:1) are shown in Fig. 4. Also shown there are spectra from the vesicles after saturation with IgG.

The spectra from the bound vesicles represent primarily free FG_3P on the inner lipid monolayer. The contribution of bound hapten is difficult to assess accurately. It is small within 10 nm of the excitation and emission maxima, which occur at 497 nm and 519 nm for spectra from both bound and unbound vesicles. In these regions the fractional quenching is independent of wavelength to within 3% (see insets showing intensity ratios in Fig. 4). For most purposes the residual fluorescence of bound haptens can be neglected; this is discussed more fully later.

Kinetics of IgG binding: dependence on phospholipid composition of vesicle

Fig. 5 shows the kinetics of the binding of excess IgG to haptenated vesicles prepared from a variety of phosphatidylcholines (DPPC, DMPC, DEPC, DOPC, POPC, egg PC, and DPhPC) and to sodium fluorescein. The relative rates of quenching are DPhPC < egg PC ≈ DOPC ≈ DEPC < POPC < DPPC < DMPC < sodium fluorescein. The quenching kinetics appears to be biphasic, and this is most pronounced for the unsaturated (DEPC, DOPC, POPC, egg PC) and branched (DPhPC) phospholipids.

The equilibrium quenching Q_{eq}, or ratio of final to initial fluorescence intensity at equilibrium, is given in Table II for each preparation from Fig. 5. We deemed that equilibrium had been attained after 30–60 min of incubation with antibody, de-

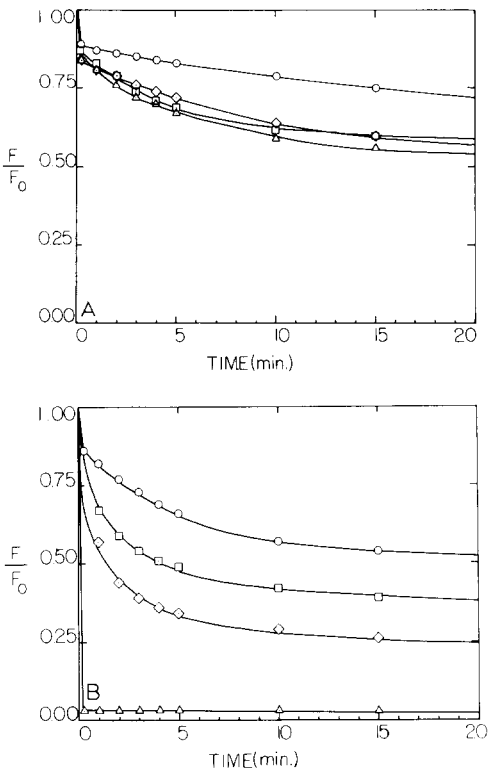

Fig. 5. Effect of vesicle lipid composition on binding kinetics of IgG to haptenated vesicles. Conditions are antibody excess (44 nM; FG_3P is at 2.8 nM). Curves are hand drawn through data points here and in subsequent figures depicting kinetics. (A) DPhPC (⊙), DOPC (◇), egg PC (⊡), and DEPC (△). (B) POPC (⊙), DPPC (⊡), DMPC (◇), and 1.95 nM sodium fluorescein (△).

pending on the preparation. Thereafter, the fluorescence signal often continued to decrease slowly at rates of about 2% per h. This may have been due to the last stages of antibody binding or to various technical limitations such as instrumental stability.

Membranes composed of unsaturated and branched phospholipids systematically show a smaller Q_{eq} than do those composed of saturated straight-chain phospholipids (DMPC, DPPC). The large Q_{eq} for DMPC strongly suggests that trans-bilayer flip-flop of the hapten is occurring [30]. The Q_{eq} for DPPC represents nearly complete binding of the hapten in the outer monolayers of the vesicles. At the other extreme, the small value of Q_{eq} for DPhPC reflects the low avidity of antibody for the vesicles in that preparation.

TABLE II

COMPARISON OF QUENCHING OF FG_3P IN VESICLES OF DIFFERENT LIPID COMPOSITION

Q_{eq} is the percentage of quenching of the FG_3P fluorescence when the kinetic curves in Figs. 6 and 7 reach equilibrium. Uncertainties in Q_{eq} are ±4.

Lipid	Q_{eq}
DPhPC	34
Egg PC	40
DOPC	44
DEPC	46
POPC	48
DMPC	77
DPPC	62
DPPC/cholesterol (95 : 5)	62
DPPC/cholesterol (90 : 10)	61
DPPC/cholesterol (80 : 20)	56
DPPC/cholesterol (67 : 33)	53
Sodium fluorescein	97

Kinetics of IgG binding: dependence on cholesterol

Haptenated vesicles were made with DPPC and up to 33 mol% cholesterol. Sufficient IgG was added to saturate the surfaces, and the kinetics of quenching was observed; see Fig. 6. 5 mol% cholesterol significantly enhances the rate of quenching, and only small additional increases are observed beyond 20 mol%. The inclusion of cholesterol in DMPC and DOPC vesicles also enhances the binding (results not shown).

Values of Q_{eq} for these vesicles are shown in Table II. The trend toward lower Q_{eq} with increasing cholesterol content primarily reflects the effect of cholesterol on vesicle size. Larger vesicles have a smaller fraction of their haptens in the outer monolayer.

Comparative binding kinetics of IgG and Fab

The binding kinetics of IgG and Fab added to suspensions of haptenated vesicles made from DPPC or DPPC/cholesterol (2 : 1) are shown in Fig. 7. Although binding-site concentrations were equal in the IgG and Fab preparations, IgG quenched hapten fluorescence more rapidly in both membranes than did Fab.

Equilibrium binding of IgG and Fab to haptenated vesicles

Equilibrium quenching data from haptenated

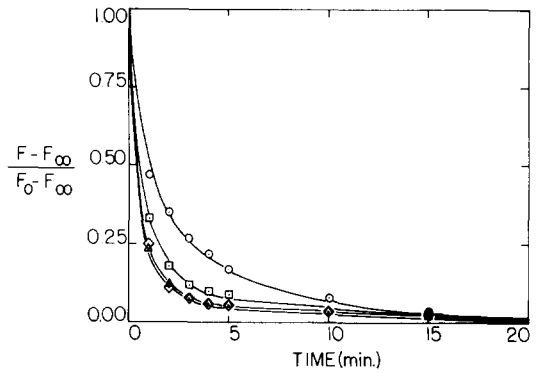

Fig. 6. Effect of cholesterol content on binding kinetics of IgG to haptenated vesicles. Conditions are saturation of vesicle surfaces with IgG (44 nM) at equilibrium (i.e., infinite time); FG_3P concentration is 2.8 nM. Fluorescence is plotted as fraction of quenchable fluorescence. Vesicles contain DPPC with following mole percentages of cholesterol: 0 (⊙), 5 (⊡), 20 (◇), and 33 (△).

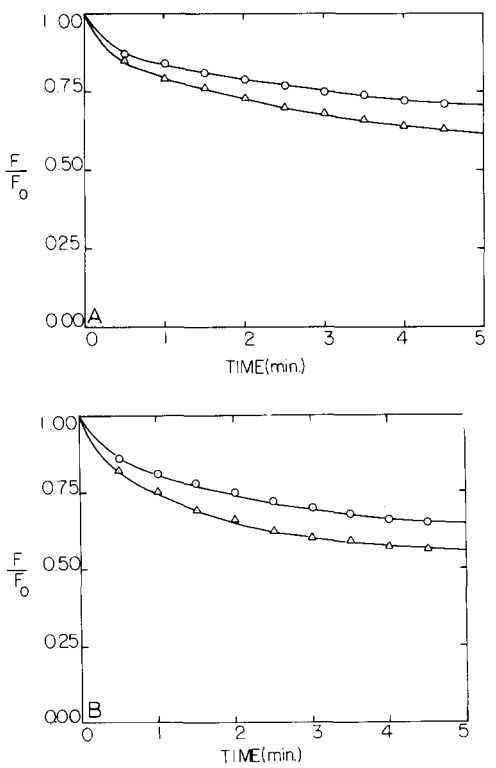

Fig. 7. Comparative kinetics of the binding of IgG (△) and Fab (⊙) to vesicles made of DPPC (A) and DPPC/cholesterol (2:1) (B). IgG and Fab concentrations were 14 nM; FG_3P concentration was 2.8 nM.

vesicles made from DOPC, DPPC, and DPPC/cholesterol (2:1) and incubated with IgG or Fab are shown in Fig. 8.

The interaction between Fab and the haptens on the vesicles is well fitted mathematically be Reaction 1, where F is now interpreted as FG_3P molecules on the outer monolayer of the vesicles. The affinity constants obtained by fitting these curves as before are shown in Table III. The quenching curves for the binding of IgG are not well fit by the same procedure. Given the potential for the bivalent IgG to cross-link haptens on vesicles, Reaction 1 is not appropriate, so this result is not surprising. A rough measure of the avidity of IgG binding is the reciprocal of the concentration of free IgG at which half of the available haptens are bound (it would equal the affinity constant if Reaction 1 were obeyed); see Table III.

The important points here are (1) the strength of both Fab and IgG interactions with the membranes varies considerably, in the order DOPC < DPPC < DPPC/cholesterol (2:1); (2) Fab always binds to the membranes more weakly than IgG; (3) the differential in IgG and Fab binding strengths is greatest for the most weakly-binding case (DOPC); and (4) the affinity of Fab for hapten on DPPC/cholesterol (2:1) vesicles is close to its affinity for sodium fluorescein.

Agglutination of vesicles

Neither of two tests detected agglutination of

TABLE III

APPARENT AVIDITIES OF IgG AND AFFINITIES OF Fab FOR HAPTENATED VESICLES OF DIFFERENT LIPID COMPOSITION

This table was constructed by analyzing the quenching curves in Fig. 8. IgG avidities are the reciprocals of the concentration of free IgG that reduced the quenchable fluorescence in the samples by one half. The Fab affinities were obtained from a least-squares fit according to Reaction 1. Experimental uncertainties are at the 95% confidence level assuming the best-fit value of B_t from Table I.

Lipid composition	K_{Fab} (M^{-1}) ($\times 10^{-8}$)	K_{IgG} (M^{-1}) ($\times 10^{-8}$)
DOPC	0.13 ± 0.03	3.0 ± 1.0
DPPC	1.2 ± 0.3	7.0 ± 2.0
DPPC/cholesterol (2:1)	4.00 ± 1.15	14.0 ± 5.0

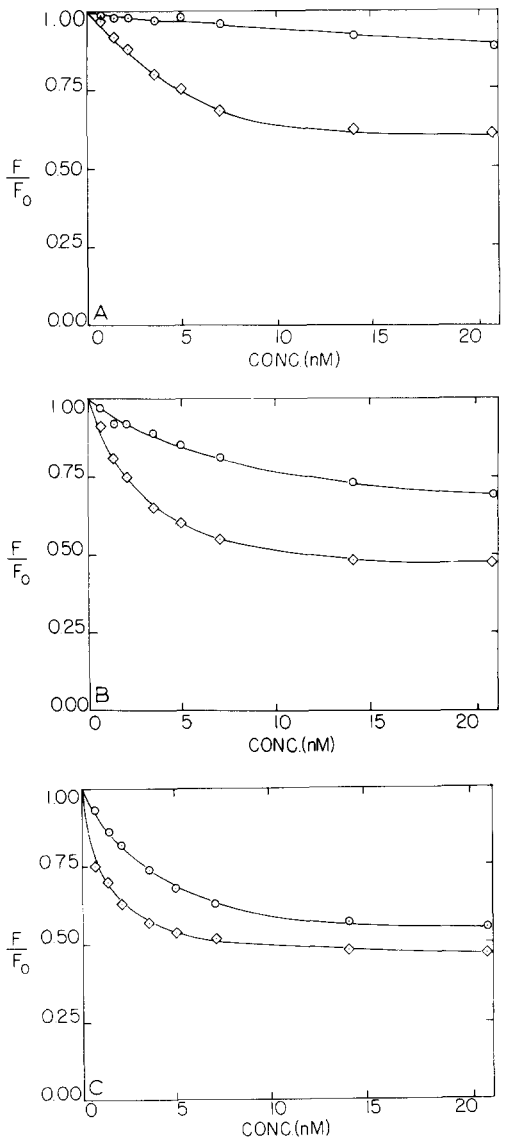

Fig. 8. Equilibrium binding of IgG (◇) and Fab (○) to haptenated vesicles made of DOPC (A), DPPC (B), and DPPC/cholesterol (2:1) (C). The abcissas show IgG or Fab concentration. The FG_3P concentration was 2.8 nM. The curves through the Fab points are the computed fits (see text and Table III); those through IgG points are hand drawn.

vesicles by IgG under our experimental conditions. The first tested the dependence of the binding kinetics on vesicle concentration; deviations from linearity would suggest agglutination. In fact, the dependence was linear to within 3% for a 5-fold variation of vesicle concentration (0.5 and 2.5 nM FG_3P at 0.1 mol% in DPPC/cholesterol (2:1) vesicles with antibody excess). The second test was to monitor light scattering, which is greatly increased by agglutination [39]. Light scattering in the above preparations was constant over the time-course of the quenching, which was essentially complete after 10 min.

Discussion

Relationship between hapten binding and fluorescence quenching

For a quantitative analysis of hapten binding, one must know the fluorescence in both the unbound and bound states. This is easy to determine for sodium fluorescein, where saturation with antibody quenches 97% for excitation and emission wavelengths near the fluorescein maxima. Both a reduction in intensity and a red-shift of the excitation and emission spectra of the bound hapten contribute to this observation [28].

The quenching should be less complete for FG_3P, for two reactions [30]: (1) the spectra of the unbound probe are already red-shifted from the sodium fluorescein positions, and (2) the high hapten pK_a will cause a lower intensity in the unbound case for some preparations, due to the presence of some mono-anionic hapten. The experimental determination of the intensity of the bound hapten is not straightforward, since an unknown fraction of the haptens is on monolayers that face the insides of the vesicles; this fraction will depend on the distribution of vesicle size and number of lamellae, as well as the amount of symmetry in the distribution of the hapten across the bilayer.

This difficulty can be circumvented by assuming that the fluorescence spectra of FG_3P and sodium fluorescein are identical when the molecules are bound by antibody, and that the spectra of the two free haptens have the same shape (though that of FG_3P is red-shifted). We then estimate that the degree of quenching of an FG_3P by antibody is 95–96% under our assay conditions.

Dependence of antibody-hapten interaction on vesicle compositions

The kinetic and equilibrium properties of the

interaction of IgG and Fab with FG_3P depend strongly on the composition of the membranes into which the hapten is incorporated. The nature of the acyl chain is important in pure phosphatidylcholine vesicles, with unsaturated and branched chains causing less binding than saturated. Incorporation of cholesterol into the membranes enhances binding.

Are these observations related to membrane 'fluidity'? In terms of lipid lateral mobility and chain conformational disorder, all of the pure PC membranes except DPPC were fluid at the experimental temperature (25 °C). For PC/cholesterol mixtures the phase behavior is complicated [40,41], but DPPC/cholesterol (2 : 1) must be considered fluid. One would expect the effects of hapten lateral mobility to show up (if at all) in the kinetics binding of IgG, specifically in the rate of conversion of monovalently to bivalently bound IgG. Hapten mobility should not affect equilibrium binding in liposomal systems such as ours, since even in 'solid' membranes lipid diffusion is fast enough to redistribute the haptens extensively on the experimental time scale.

We have in fact found no simple correlation between membrane fluidity and any aspect of antibody binding that we have studied. Moreover, we observe qualitatively the same compositional effects on Fab and IgG binding. Apparently, differences in hapten lateral mobility among our systems affect antibody binding less than some other factors that are unrelated to lateral diffusion and multivalent binding.

We hypothesize that the hapten exists in at least two interconvertible states, (1) extended away from the membrane, where it is available for antibody binding, and sequestered at or in the membrane surface, where it is cryptic. In the simplest case, the binding of antibody to the extended hapten is independent of vesicle lipid composition; the avidity of the antibody for the vesicle decreases as the amount of sequestered hapten increases. This affects only the numerical values of calculated affinity and avidity constants and not the functional form of the equilibrium binding, as long as an equilibrium is maintained between the extended and sequestered states [42], (Owicki, J. and Petrossian, A., manuscript in preparation).

The shapes of the curves for antibody-binding kinetics support the existence of extended and sequestered haptens. Especially for the weakly binding compositions at high IgG concentrations, the curves are distinctly biphasic: a fast initial binding is followed by a slower process. For antibody excess, the kinetic equations generated by the extended-sequestered model indeed indicate that the fluorescence quenching should be the sum of two exponential processes. When binding of extended hapten by antibody is much faster than the rate of conversion of sequestered to extended hapten, the two quenching steps can be identified with these two molecular processes.

That at least some of the hapten is extended is demonstrated by the ability of the antibody to bind FG_3P (but not fluorescein-PE). Direct spectroscopic evidence of the existence of multiple hapten environments is presented in this paper's companion [30]. In a future paper we will examine the binding kinetics and hapten availability in more detail.

The crypticity that we have observed may be biologically significant, particularly in its modulation by cholesterol. Although its role is controversial, cholesterol is an important component of biological systems [43]. Alterations of serum or membrane cholesterol content have been associated with two of the most important human pathologies, atherosclerosis [44,45] and neoplasia [46,47], both of which exhibit abnormalities of recognition or proliferation. In one study, increases in antigenicity of transformed cells were observed after the incorporation of cholestenyl hemisuccinate [48]. It remains to be seen whether similar mechanisms operate in our model system and the biological ones.

Effects of bivalency

Conditions for multivalent binding to target surfaces are of interest both because multivalent binding is stronger than monovalent [49,50] and because there is evidence that other components of the immune system recognize and are triggered preferentially by multivalently bound antibodies [51,52]. IgG bound more strongly than Fab fragments to all membranes studied here, which is presumptive evidence of bivalent attachment. Bivalent binding has been reported in related liposomal systems [53,54]. Our result is different from

that of Mason and Williams [55], who emphasized the importance of monovalent binding of monoclonal antibodies to cell-surface antigens on rat thymocytes.

The enhancement of binding due to bivalency is clear but not dramatic. When the second antibody foot binds a hapten, there are costs in free energy due to steric effects and entropic restrictions. In this system, these costs apparently come close to balancing the gains due to doubling the intermolecular interactions in the antibody-hapten binding sites. The high surface curvature of the rather small vesicles that we used may have contributed to this. The vesicle diameters were only about three times the maximum distance between binding sites on an IgG, assuming flexibility at the hinge region of the antibody.

There was negligible agglutination of vesicles, a result opposite that observed in a similar system by Luedtke and Karush [56]. The difference may be mostly in the experimental conditions: our vesicle concentrations were 30- to 600-times lower than theirs, and we worked at antibody excess rather than near antibody-hapten equivalence.

Conclusions

We have synthesized the conjugate of a highly fluorescent hapten, fluorescein, to the headgroup of a phospholipid. Incorporated into liposomes and allowed to interact with anti-fluorescein antibodies, this forms a sensitive and convenient model system for analyzing problems in immunological recognition.

We have determined that, depending on liposome composition, some of the hapten is sequestered at the membrane surface and is unavailable for antibody binding. The presence of cholesterol in the membrane greatly reduced this effect, an observation that may be biologically important. Since hapten-membrane associations have been seen in related systems [31,42,56], they appear to be a common feature of haptenated liposomes. They must be taken into account before other effects, such as hapten lateral mobility, can be studied.

We have shown that the affinity of monovalent Fab fragments for haptens on the liposomes can approach that for the haptens in aqueous solution, if the liposomal haptens are not strongly sequestered. Finally, we have shown that IgG can bind bivalently to the haptenated vesicles even though in this study the vesicles were small and highly curved.

Acknowledgements

We are pleased to thank E.W. Voss, Jr., for the generous gift of his hybridoma line. We are grateful to R. Reginato for doing the mass spectroscopy, and to A.L. Burlingame, Director of the Bio-organic Biomedical Mass Spectrometry Resource, which is supported by NIH Division of Research Resources Grant RR01614. We also acknowledge valuable conversations with A. Kantor and S. Stanton. A.P. is a Neshan Zovick fellow. This work was supported by the following grants: N.I.H. R01-AI-19605-02, L.B.L. Director's Funding, U.C. Cancer Res. Coord. Comm. Grant 80B2, and B.R.S.G. Grant 2-S07-RR-7006 from the Biomedical Research Support Program, N.I.H.

Reference

1 Papahadjopoulos, D. (ed.) (1978) Liposomes and Their Uses in Biology and Medicine, Ann. N.Y. Acad. Sci., Vol. 308
2 Gregoriadis, G. and Allison, A.C. (eds.) (1980) Liposomes in Biological Systems John Wiley and Sons, New York
3 Baldwin, T.H. and Howard, S.R. (eds.) (1980) Liposomes and Immunobiology, Elsevier/North Holland, Amsterdam
4 Uemura, K., Nicolotti, R.A., Six, H.R. and Kinsky, S.C. (1974) Biochemistry 13, 1572–1578
5 Parce, J.W., Kelley, D. and Heinzelmann, K. (1983) Biochim. Biophys. Acta 736, 92–98
6 Balakrishnan, K., Hsu, F.J., Cooper, A.D. and McConnell, H.M. (1982) J. Biol. Chem. 257, 6427–6433
7 Hakomori, S. (1981) Annu. Rev. Biochem. 50, 733–764
8 Hakomori, S., Stellner, K. and Watanabe, K. (1972) Biochem. Biophys. Res. Commun. 49, 1061–1068
9 Van Heyningen, W.E. (1974) Nature 249, 415–417
10 Yogeeswaran, G. (1983) Adv. Cancer Res. 38, 289–350
11 Ryan, J.L. and Shinitzky, M. (1979) Eur. J. Immunol. 9, 171–175
12 Wang, T.J., Freimuth, W.W., Miller, H.C. and Esselman, W.J. (1978) J. Immunol. 121, 1361–1365
13 Esselman, W.J. and Miller, H.C. (1977) J. Immunol. 119, 1994–2000
14 Higgins, T.J., Sabatino, A.P., Remold, H.G. and David, J.R. (1978) J. Immunol. 121, 880–886
15 Lengle, E.E., Krishnaraj, R. and Kemp. R.G. (1979) Cancer Res. 39, 817–822
16 Poste, G. and Kirsh, R. (1983) Biotechnology 1, 869–878

17 Godfrey, W., Doe, B. and Wofsy, L. (1983) Proc. Natl. Acad. Sci. USA 80, 2267–2271
18 Hashimoto, Y., Sugawara, M., Masuko, T. and Hojo, H. (1983) Cancer Res. 43, 5328–5334
19 Gabizon, A., Goren, D., Fuks, Z., Barenholz, Y., Dagan, A. and Meshorer, A. (1983) Cancer Res. 43, 4730–4735
20 Alving, C.R., Joseph, K.C., Lindsley, H.B. and Schoenbechler, M.J. (1974) Proc. Soc. Exp. Biol. Med. 146, 458–461
21 Humphries, G.M.K. and McConnell, H.M. (1974) Proc. Natl. Acad. Sci. USA 71, 1691–1694
22 Boggs, J.M., Samji, N., Moscarello, M.A., Hashim, G.A. and Day, E.D. (1983) J. Immunol. 130, 1687–1694
23 Voss, E.W., Jr., Eschenfeld, W. and Root, R.T. (1976) Immunochemistry 13, 447–453
24 Dandliker, W.B., Schapiro, H.C., Meduski, J.W., Alonso, R., Feigen, G.A. and Hamrick, J.R., Jr. (1964) Immunochemistry 1, 165–191
25 Lopatin, D.E. and Voss, E.W., Jr. (1971) Biochemistry 10, 208–213
26 Parker, C.W. (1978) in Handbook of Experimental Immunology, 3rd Edn., Vol. 1, Chapt. 18 (Weir, D.M., ed.), Blackwell Scientific, Oxford
27 Kranz, D.M. and Voss, E.W., Jr. (1981) Mol. Immunol. 18, 889–898
28 Kranz, D.M., Herron, J.N. and Voss, E.W., Jr. (1982) J. Biol. Chem. 257, 6987–6995
29 Kranz, D.M. and Voss, E.W., Jr. (1983) Mol. Immunol. 20, 1301–1312
30 Stanton, S., Kantor, A., Petrossian, A. and Owicki, J.C. (1984) Biochim. Biophys. Acta 776, 228–236
31 Brûlet, P. and McConnell, H.M. (1977) Biochemistry 16, 1209–1217
32 Dancey, G.F., Isakson, P.C. and Kinsky, S.C. (1979) J. Immunol. 122, 638–642
33 Potter, M., Pumphrey, J.G. and Walters, J.L. (1972) J. Natl. Cancer Inst. 49, 305–308
34 Hoogenraad, N., Helman, T. and Hoogenraad, J. (1983) J. Immunol. Methods 61, 317–320
35 Langone, J.J. (1982) J. Immunol. Methods 55, 277–296
36 Porter, R.R. (1959) Biochem. J. 73, 119–126
37 Batzri, S. and Korn, E.D. (1973) Biochim. Biophys. Acta 298, 1015–1019
38 Kremer, J.M.H., Van de Esker, M.W.J., Pathmamanoharan, C. and Wiersema, P.H. (1977) Biochemistry 16, 3932–3935
39 Alecio, M.R. and Rando, R.R. (1982) J. Membrane Biol. 67, 137–141
40 Rubenstein, J.L.R., Owicki, J.C. and McConnell, H.M. (1980) Biochemistry 19, 569–573
41 Recktenwald, D.J. and McConnell, H.M. (1981) Biochemistry 20, 4505–4510
42 Balakrishnan, K., Mehdi, S.Q. and McConnell, H.M. (1982) J. Biol. Chem. 257, 6434–6439
43 Jain, M.K. (1975) Curr. Topics Membranes Transport 6, 1–57
44 Jackson, R.L. and Gotto, A.M. (1976) in Atherosclerosis Reviews, Vol. 1, pp. 1–21, Raven Press, New York
45 Kannel, W.B., Castelli, W.P. Gordon, T. and McNamara, P.M. (1971) Ann. Intern. Med. 74, 1–12
46 Chen, H.W., Kandutsch, A.A. and Heiniger, H.J. (1978) Prog. Exp. Tumor Res. 22, 275–316
47 Coleman, P.S. and Lavietes, B.B. (1981) CRC Critical Reviews in Biochemistry, 341–393
48 Shinitzky, M. and Skornick, Y. (1982) in Membranes in Tumor Growth (Galeotti, T., Cittadini, A., Neri, G. and Papa, S., eds.), pp. 61–68, Elsevier Biomedical Press, Amsterdam
49 Karush, F. (1970) Ann. N.Y. Acad. Sci. 169, 56–64
50 Crothers, D.M. and Metzger, H. (1972) Immunochemistry 9, 341–357
51 Parce, J.W., Henry, N. and McConnell, H.M. (1978) Proc. Natl. Acad. Sci. USA 75, 1515–1518
52 Pecht, I., Ehrenberg, B., Calef, E. and Arnon, R. (1977) Biochem. Biophys. Res. Commun. 74, 1302–1310
53 Parce, J.W., Schwartz, M.A., Owicki, J.C. and McConnell, H.M. (1979) J. Phys. Chem. 83, 3414–3417
54 Kobayashi, M., Nakanishi, M. and Tsuboi, M. (1982) J. Biochem. 91, 407–409
55 Mason, D.W. and Williams, A.F. (1980) Biochem. J. 187, 1–20
56 Luedtke, R. and Karush, F. (1982) Biochemistry 21, 5738–5744